
Journal of Coordination Chemistry
Publication details, including instructions for authors and subscription information:
http://www.tandfonline.com/loi/gcoo20

# Heterocyclic substituted thiosemicarbazides and their Cu(II) complexes: synthesis, spectral characterization, thermal, molecular modeling, and DNA degradation studies

O.A. El-Gammal [a], G.M. Abu El-Reash [a], S.E. Ghazy [a] & T. Yousef [b]

[a] Department of Chemistry, Faculty of Science, Mansoura University, Mansoura 35516, Egypt

[b] Department of Toxic and Narcotic Drug, Forensic Medicine, Mansoura Laboratory, Medicolegal Organization, Ministry of Justice, Egypt

Published online: 05 Apr 2012.

To cite this article: O.A. El-Gammal, G.M. Abu El-Reash, S.E. Ghazy & T. Yousef (2012) Heterocyclic substituted thiosemicarbazides and their Cu(II) complexes: synthesis, spectral characterization, thermal, molecular modeling, and DNA degradation studies, Journal of Coordination Chemistry, 65:10, 1655-1671, DOI: 10.1080/00958972.2012.674519

To link to this article: http://dx.doi.org/10.1080/00958972.2012.674519

*Journal of Coordination Chemistry*
Vol. 65, No. 10, 20 May 2012, 1655–1671



# Heterocyclic substituted thiosemicarbazides and their Cu(II) complexes: synthesis, spectral characterization, thermal, molecular modeling, and DNA degradation studies

O.A. EL-GAMMAL*†, G.M. ABU EL-REASH†, S.E. GHAZY† and T. YOUSEF‡

†Department of Chemistry, Faculty of Science, Mansoura University, Mansoura 35516, Egypt
‡Department of Toxic and Narcotic Drug, Forensic Medicine, Mansoura Laboratory, Medicolegal Organization, Ministry of Justice, Egypt

(*Received 10 August 2011; in final form 17 February 2012*)

Four Cu(II) complexes of $N^1$-phenyl-$N^2$-(pyridin-2-yl)hydrazine-1,2-bis(carbothioamide) ($H_2$PPS), *N*-phenyl-2-(2-(pyridin-2-ylcarbamothioyl)hydrazinyl)-2-thioxoacetamide ($H_2$PBO), *N*-phenyl-2-(pyridin-2-ylcarbamothioyl)hydrazinecarboxamide ($H_2$APO), and 1-(amino*N*-(pyridin-2-yl)methanethio)-4-(pyridin-yl)thiosemicarbazide ($H_2$PPY) have been prepared and characterized by elemental analyses, spectral (infrared (IR), UV-Visible, $^1$H NMR, and electron spin resonance (ESR)) as well as magnetic and thermal measurements. Varying the substituents on the thiosemicarbazide led to remarkable modifications of the mode of coordination. IR spectral data reveal that the ligands are SN bidentate, NON tridentate, or NSNS tetradendate chelates forming structures in which copper is square-planar or octahedral. ESR spectra of these complexes are quite similar and exhibit an axially symmetric *g*-tensor parameter with $g_{\parallel} > g_{\perp} > 2.0023$ revealing an appreciable covalency with $d_{(x^2-y^2)}$ as the ground-state. Bond lengths, bond angles, HOMO, LUMO, and dipole moments have been calculated to confirm the geometry of the thiosemicarbazide derivatives and their corresponding complexes. Proton-ligand dissociation and copper-ligand stability constants of all ligands were calculated pH-metrically. The effect of the compounds on calf thymus DNA was investigated.

*Keywords*: Heterocyclic thiosemicarbazides; Copper(II) complexes; Thermal degradation; Calf thymus DNA



## 1. Introduction

Thiosemicarbazones are sulfur ligating systems with a range of biological properties [1–4]. Thiosemicarbazide syntheses can be modified from the parent aldehyde or ketone, or by substitution at $^2$C or $^1$N [5–7]. Thiosemicarbazide complexes have anticancer and antimicrobial activity owing to their ability to diffuse through the semipermeable membrane of cell lines [5, 8–10]. The biological activity of copper, a metal that plays an important role in many biological processes [11], has been the subject of numerous studies [12–14]. Since Sigman *et al.* [15] discovered in 1979 that

*Corresponding author. Email: olaelgammal@yahoo.com


ISSN 0095-8972 print/ISSN 1029-0389 online 
http://dx.doi.org/10.1080/00958972.2012.674519

copper ions complexed to 1,10-phenanthroline were capable of cleaving DNA [16], copper complexes with a nitrogen donor heterocyclic ligand have been used widely to improve nuclease activity [17–21], mostly because of their ability to break the DNA chain in the presence of $H_2O_2$ and reducing agents [22]. In this work, we study the coordination chemistry of substituted thiosemicarbazides, $N^1$-phenyl-$N^2$-(pyridin-2-yl)hydrazine-1,2-bis(carbothioamide) ($H_2PPS$), *N*-phenyl-2-(pyridin-2-ylcarbamothioyl) hydrazinecarboxamide ($H_2PBO$), 1-(amino(thioformyl)-*N*-phenylform) -4-(pyridin-2-yl)thiosemicarbazide ($H_2APO$), and 1-(amino*N*-(pyridin-3-yl)methanethio)-4-(pyridin-yl)thiosemicarbazide ($H_2PPY$) to correlate their structures with their ability to degrade DNA.



## 2. Experimental

### 2.1. *Materials and physical measurements*

All chemicals were purchased from Aldrich and Fluka and used without purification. Elemental analyses (C, H, and N) were performed on a Perkin-Elmer 2400 analyzer. All compounds were within ±0.5% of the theoretical values. Melting points were determined in open capillaries on an electrothermal melting point apparatus (Electrothermal Engineering Ltd., Essex, UK) and are uncorrected. $^1$H NMR spectra were recorded in DMSO-$d_6$ on a JEOL JNM LA 300 WB spectrometer at 300 MHz using TMS (tetramethylsilane) as an internal standard (chemical shift in $\delta$ ppm) and the infrared (IR) spectra of the ligands were recorded as KBr discs on a Mattson 5000 FTIR spectrophotometer. Magnetic susceptibilities were measured with a Sherwood scientific magnetic susceptibility balance at 298 K. Thermogravimetric measurements (TGA, DTA, 20–1000°C) were recorded on a DTG-50 Shimadzu thermogravimetric analyzer at a heating rate of 10°C min$^{-1}$ and nitrogen flow rate of 20 mL min$^{-1}$. Electron spin resonance (ESR) spectra were obtained on a Bruker EMX spectrometer working in the X-band (9.78 GHz) mode with 100 kHz modulation frequency. The microwave power and modulation amplitudes were set at 1 mW and 4 Gauss, respectively. The low field signal was obtained after four scans with 10-fold increase in the receiver gain. A powder spectrum was obtained in a 2 mm quartz capillary at room temperature.

### 2.2. *Synthesis of the ligands*

4-(2-Pyridyl)-3-thiosemicarbazide (**1**) was synthesized as reported earlier [23]. Derivatives (**2**–**5**) were prepared by heating ethanolic solution of 4-(2-pyridyl)-3-thiosemicarbazide (**1**) (1.6 g, 100 mmol) with an equimolar amount of phenyl isothiocyanate, phenyl isocyanate, benzoyl isothiocyanate, and 2-pyridyl isothiocyanate, respectively.

**2.2.1. $H_2PPS$ (2).** Yield 78%; m.p.: 178–180°C, $C_{13}H_{13}N_5S_2$ (303.41): Calcd C 51.46, H 4.32, N 23.08, S 21.14; found C 51.13, H 4.25, N 22.96, S 21.11. IR (KBr): $\nu/\delta = 1223$,

850 (C=S), 3099 $(NH)_{a,a'}$, 3160 $(NH)_{b,c}$, 1569 $(C{=}N)_{py}$, and 1598 (C=C). $^1$H NMR $\delta = 15.4$ (s,1H,SH), 11.10, 10.97 (s,1H,$NH_{a,a'}$), 8.27, 8.25 (d, $J = 1.2$ Hz,1H,$NH_{b,c}$), 8.26 (d, $J = 5.4$ Hz, 1H, pyridine $H_6$), 7.85 (dd, $J = 6.9$, 5.4 Hz, 1H, pyridine H4), 7.65 (dd, $J = 6.9$, 4.8 Hz, 1H, pyridine H5), 7.37–7.50 (d, $J = 5.4$ Hz, 1H, pyridine H3), 7.00–7.35 (m, 5H, Ph ring).

**2.2.2. $H_2$PBO (3).** Yield 79%; m.p.: 267–270°C, $C_{14}H_{13}N_5OS_2$ (331.42): Calcd C 50.74, H 3.95, N 21.13, O 4.83, S 19.35; found C 50.35, H 3.47, N 21.78, O 4.71, S 19.31. IR (KBr): $\nu/\delta = 1243$, 865 (C=S), 3158, 3100 $(NH)_{a,a'}$, 3239 $(NH)_{b,c}$, 1542 $(C{=}N)_{py}$, 1675 (C=O), and 1604 (C=C). $^1$H NMR $\delta = 11.09$, 10.53 (s,1H,$NH_{a,a'}$), 9.54, 8.20 (d,1H,$NH_{b,c}$), 8.27 (d, $J = 8.1$ Hz, 1H, pyridine H3), 2 (d, $J = 5.1$ Hz, 1H, pyridine H6), 7.55 (dd, $J = 6.3$, 5.7 Hz, 1H, pyridine H4), 7.78 (dd, $J = 7.5$, 6.3 Hz, 1H, pyridine H5), 7.12–7.23 (m, 5H, Ph ring).

**2.2.3. $H_2$APO (4).** Yield 81%; m.p.: 180–182°C, $C_{13}H_{13}N_5OS$ (287.34): Calcd C 54.34, H 4.56, N 24.37, O 5.57, S 11.16; found C 54.15, H 4.45, N 23.98, O 5.78, S 11.11. IR (KBr): $\nu/\delta = 1247$, 800 (C=S), 3170, 3104 $(NH)_{a,a'}$, 3220 $(NH)_{b,c}$, 1641 $(C{=}N)_{py}$, 1672 (C=O), and 1600 (C=C). $^1$H NMR: $\delta = 15.8$ (s,1H,SH), $\delta = 11.9$, 11.30 (s,1H,$NH_{a,a'}$), 8.36, 8.09 (d,1H,$NH_{b,c}$), 8.23 (dd, $J = 8.7$, 6 Hz, 1H, pyridine H5), 8.01 (d, $J = 5.3$ Hz, 1H, pyridine H6), 7.9 (d, $J = 6.4$ Hz, 1H, pyridine H3), 7.66 (dd, $J = 6.1$, 4.8 Hz, 1H, pyridine H4), 7.0–7.64 (m, 5H, Ph ring).

**2.2.4. $H_2$PPY (5).** Yield 82%; m.p.: 307–310°C, $C_{12}H_{12}N_6S_2$ (304.06): Calcd C 47.35, H 3.97, N 27.61, S 21.07; found C 47.02, H 4.05, N 27.86, S 21.31. IR (KBr): $\nu/\delta = 1218$, 875 (C=S), 3174 $(NH)_{a,a'}$, 3234 $(NH)_{b,c}$, 1562 $(C{=}N)_{py}$, and 1604 (C=C). $^1$H NMR $\delta = 15.4$ (s,1H,SH), 11.10 (s,1H,$NH_{a,a'}$), 8.29, 8.28 (d, $J = 3.9$, 1H, $NH_{b,c}$), 8.21 (d, $J = 6.2$ Hz, 1H, pyridine H6), 8.17 (d, $J = 7.4$ Hz, 1H, pyridine H3), 7.88 (dd, $J = 5.5$, 3.3 Hz, 1H, pyridine H5), 7.85 (dd, $J = 6.6$, 5.4 Hz, 1H, pyridine H4).

### 2.3. *Synthesis of Cu(II) complexes*

Ethanolic solution of thiosemicarbazides (1.0 mmol) and hydrated copper chloride (1.0 mmol) was refluxed for 2–3 h. The precipitates that formed were filtered off, washed with hot ethanol followed by diethyl ether, and dried in a vacuum desiccator over anhydrous $CaCl_2$. The complexes have high melting points and are insoluble in common organic solvents and soluble in DMF or DMSO.

**2.3.1. [Cu(HPPS)Cl($H_2O$)$_2$] (6).** Anal. Calcd for $C_{13}H_{14}CuN_5OS_2Cl$: C 37.23, H 3.36, N 16.69, S 15.29, Cu 15.2, Cl 8.45; Found: C 37.59, H 3.18, N 17.05, S 15.43, Cu 15.4, Cl 8.15. Main IR peaks (KBr, $cm^{-1}$): $\nu(NH)_{a,a'}$ 3120, 3070; $\nu(NH)_{b,c}$ 3230; $\nu(C{=}N)_{py}$ 1616; $\nu/\delta$ $(C{=}S)_{a,a'}$ 1232, 860; $\nu$(C=N)* 1600; $\nu$(C–S) 646; UV-Vis (DMF, $cm^{-1}$) 35,211.

**2.3.2. [Cu(HPBO)Cl($H_2O$)$_2$] (7).** Anal. Calcd for $C_{14}H_{16}CuN_5O_3S_2Cl$: C 36.12, H 3.46, N 15.04, S 13.77, Cu 13.6, Cl 4.61; Found: C 36.33, H 3.78, N 15.55, S 13.48, Cu 13.4, Cl 7.81. Main IR peaks (KBr, $cm^{-1}$): $\nu(NH)_{a,a'}$ 3187; $\nu$(C=O) 1673; $\nu(C{=}N)_{py}$

1562; $\nu/\delta$ (C=S)$_{a,a'}$ 1221, 854; $\nu$(C=N)* 1612; $\nu$(C–S) 646; UV-Vis (DMF, $cm^{-1}$) 32,258; 28,409; 18,050.

**2.3.3. [Cu(HAPO)Cl](H$_2$O) (8).** Anal. Calcd for $C_{13}H_{18}CuN_5O_4SCl$: C 35.54, H 4.13, N 15.04, S 13.77, Cu 14.50, Cl 8.10; Found: C 35.66, H 4.05, N 15.55, S 13.48, Cu 14.45, Cl 8.30. Main IR peaks (KBr, $cm^{-1}$): $\nu$(NH)$_{a,a'}$ 3244; $\nu$(NH)$_{b,c}$ 3115; $\nu$(C=N)$_{py}$ 1621; $\nu/\delta$ (C=S)$_{a,a'}$ 1232, 865; $\nu$(C=N)* 1567; UV-Vis (DMF, $cm^{-1}$) 35,211; 32,467; 27,624; 23,585; 19,685; 15,291.

**2.3.4. [Cu(HPPY)Cl (H$_2$O)$_2$] (9).** Anal. Calcd for $C_{12}H_{15}CuN_6O_2S_2Cl$: C 32.84, H 3.45, N 19.16, S 14.63, Cu 14.4, Cl 8.1; Found: C 32.63, H 3.8, N 19.34, S 14.28, Cu 13.4, Cl 8.8. Main IR peaks (KBr, $cm^{-1}$): $\nu$(NH)$_{a,a'}$ 3187; $\nu$(C=N)$_{py}$ 1562; $\nu/\delta$ (C=S)$_{a,a'}$ 1221, 840; $\nu$(C=N)* 1612; $\nu$(C–S) 656; UV–Vis (DMF, $cm^{-1}$) 35,211; 31,847; 29,585; 25,126; 19,157.

### 2.4. *pH metric studies*

The experimental procedure involves pH-metric titrations of solution mixtures against standardized NaOH ($9.2 \times 10^{-3}$ mol L$^{-1}$) in 50% (v/v) dioxane-water at (298, 303, and 308 K) and at constant ionic strength of ($\mu = 0.1$, 0.15, and 0.2 mol L$^{-1}$ KCl). The solution mixtures (i–iii) were prepared as follows:

(i) 1.25 mL ($1.1 \times 10^{-2}$ mol L$^{-1}$) HCl + 1.25 mL (0.1, 0.15, and 0.2 mol L$^{-1}$) KCl + 10 mL twice-distilled $H_2O$.
(ii) 1.25 mL ($1.1 \times 10^{-2}$ mol L$^{-1}$) HCl + 1.25 mL (0.1, 0.15, and 0.2 mol L$^{-1}$) KCl + 2.5 mL ($5 \times 10^{-3}$ mol L$^{-1}$) $H_2$PPS, $H_2$PBO, $H_2$APO, and $H_2$PPY + 10 mL twice-distilled $H_2O$.
(iii) 1.25 mL ($1.1 \times 10^{-2}$ mol L$^{-1}$) HCl + 1.25 mL (0.1, 0.15, and 0.2 mol L$^{-1}$) KCl + 2.5 mL ($5 \times 10^{-3}$ $Cu^{2+}$ solution) + 0.5 mL ($5 \times 10^{-3}$ mol L$^{-1}$) metal ion in twice-distilled water + 9.5 mL $H_2O$.

The total volume was adjusted to 25 mL by adding dioxane in each case. The pH-meter readings in 50% (v/v) dioxane mixture are corrected according to the Van Uitert and Hass relation [24].

### 2.5. *DNA interaction studies*

A solution of 2 mg of calf thymus DNA (ct-DNA) was dissolved in 1 mL of sterile distilled water. Stock concentrations of the ligands and complexes were prepared by dissolving 2 mg mL$^{-1}$ in DMSO. Equal volumes from each compound and DNA were mixed thoroughly and kept at room temperature for 2–3 h. The effect of the chemicals on the DNA was analyzed by agarose gel electrophoresis. Loading dye (2 µL) was added to 15 µL of the DNA mixture before being loaded into the well of agarose gel. The loaded mixtures were fractionated by electrophoresis, visualized by UV and photographed [25].

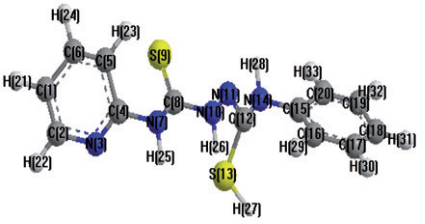


Scheme 1. Molecular modeling of $H_2PPS$.

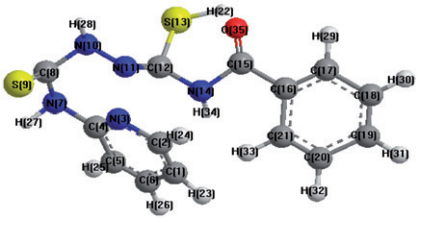


Scheme 2. Molecular modeling of $H_2PBO$.

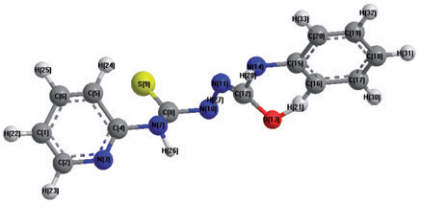

Scheme 3. Molecular modeling of $H_2APO$.

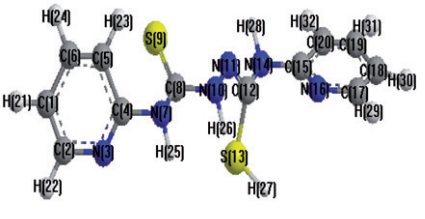


Scheme 4. Molecular modeling of $H_2PPY$.

## 2.6. *Molecular modeling*

To gain better insight on the molecular structure of the ligands (schemes 1–4) and complexes (schemes 5–8), geometric optimization and conformational analysis have been performed using MM+ [26] force field as implemented in HyperChem 8 [27].

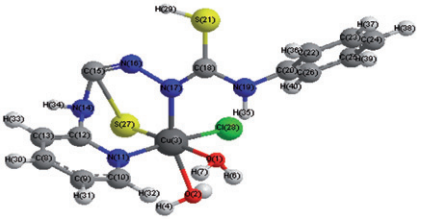

Scheme 5. Molecular modeling of $[Cu(HPPS)Cl(H_2O)_2]$ complex.

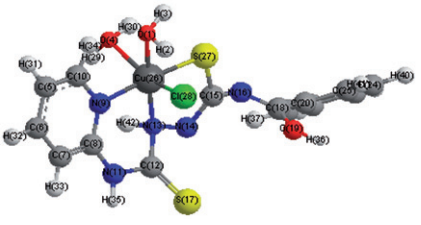

Scheme 6. Molecular modeling of $[Cu(HPBO)Cl(H_2O)_2]$ complex.

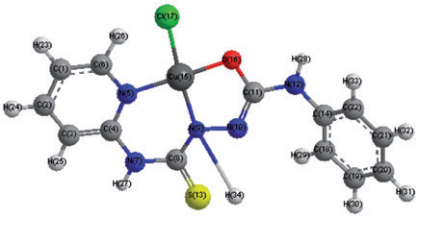

Scheme 7. Molecular modeling of $[Cu(HAPO)Cl](H_2O)$ complex.

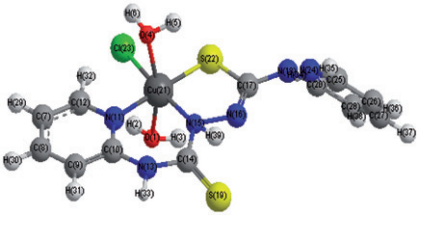

Scheme 8. Molecular modeling of $[Cu(HPPY)Cl(H_2O)_2]$ complex.

## 3. Results and discussion

### 3.1. *Synthesis and spectroscopy*

In continuation of our previous work on pyridine chemistry [28], we synthesized some new thiosemicarbazide derivatives containing the pyridine ring (scheme 9).

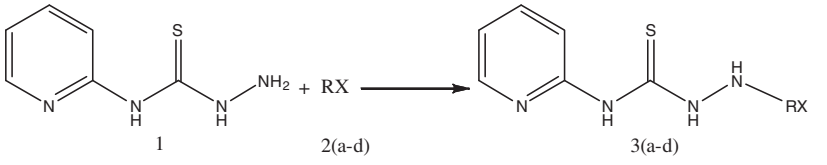


| | R | X |
|---|---|---|
| A | ph | NCS |
| B | ph | NCOS |
| C | ph | NCO |
| D | 2-py | NCS |

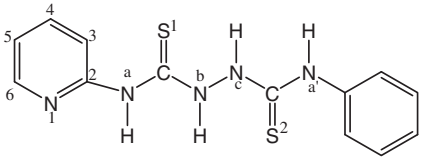

$N^1$-phenyl-$N^2$-(pyridin-2-yl)hydrazine-1,2-bis(carbothioamide)
($H_2$PPS)

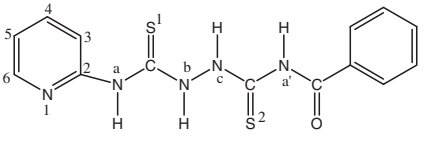

*N*-phenyl-2-(2-(pyridin-2-ylcarbamothioyl)hydrazinyl)-2-thioxoacetamide
($H_2$PBO)

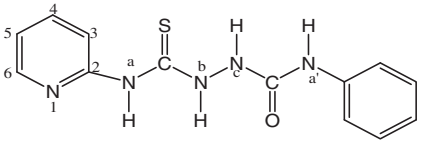

*N*-phenyl-2-(pyridin-2-ylcarbamothioyl)hydrazinecarboxamide
($H_2$APO)

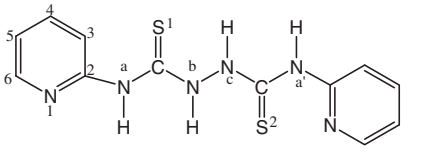

1-(amino*N*-(pyridin-2-yl)methanethio)-4-(pyridin-2-yl)thiosemicarbazide
($H_2$PPY)

Scheme 9. The synthesized thiosemicarbazide derivatives.

### 3.2. *IR spectra*

IR spectra of the free ligands show three bands in the region 3234–3100 $cm^{-1}$ attributable to stretching modes of the $(NH)_{a,a'}$ and $\nu(NH)_{b,c}$ groups. The stretching and out-of-plane ring deformation modes ($\nu/\delta$) of the pyridine ring are observed at ≈1560 and 620–635 $cm^{-1}$ [29]. Strong bands due to stretching vibration of $\nu$(C=N) (azomethine) in $H_2$PPS and $H_2$PBO thiosemicarbazides are at 1646 and 1641 $cm^{-1}$, respectively; this band was difficult to recognize in $H_2$PPY because it is overlapped with $\nu$(C=C) of the pyridine ring. The stretching and bending vibrations ($\nu/\delta$) of the C=S groups are observed as strong bands at 1218–1247 $cm^{-1}$ and 840–865 $cm^{-1}$, respectively [30, 31]. As these ligands contain two C=S groups, $(C=S)^1$ and $(C=S)^2$, we propose that $(C=S)^1$ is in the thione form and $(C=S)^2$ in the thiol form as confirmed by the existence of additional bands at ~2600 and 660 $cm^{-1}$ in the spectra of the aforementioned ligands assignable to $\nu$(C–S) and $\nu$(SH). This assumption is further supported by the absence of bands due to $\nu$(C=N) (azomethine), $\nu$(C–S), and $\nu$(SH) in the IR spectrum of the starting (4-pyridyl thiosemicarbazide) [32] and the absence of the SH signal in the $^1$H NMR spectrum of $H_2$APO.

Also, the appearance of $\delta$ (C–S) in $H_2$PPY at higher wavenumber, 683 $cm^{-1}$, than that of other ligands may be due to presence of pyridyl groups which act as electron-withdrawing groups.

In $H_2APO$, the sharp band at 3521 $cm^{-1}$ may be due to $\nu$(OH) in addition to the $\nu$(CO) band at 1675 $cm^{-1}$, suggesting the keto–enol tautomerism.

IR spectra of the investigated Cu(II) complexes show that $H_2PPS$, $H_2PBO$, $H_2APO$, and $H_2PPY$ coordinate as mono-negative tridentate through (C=N) of pyridine, N of $NH_b$, and one of the (C=S) groups adjacent to $N^4$ in the thiol form ($H_2PPS$, $H_2PBO$, and $H_2PPY$) or enolized carbonyl group in $H_2APO$.

This chelation is supported by the shift of deformation mode of the pyridine ring either to lower or higher wavenumber, indicative of coordination of the metal to pyridine [33], and the band due to thioamide(4) at 840–875 either shifts to lower wavenumber [34] or disappears with simultaneous appearance of a new band assignable to $\nu$(C–S), suggesting coordination *via* C=S either in the thione form [Cu(HPPS)Cl($H_2O$)$_2$] or the thiol form [Cu(HPBO)Cl($H_2O$)$_2$] and [Cu(HPPY)Cl($H_2O$)$_2$] [35]. The shift of $\nu$(N–N) to higher wavenumber is further evidence for coordination *via* $(NH)_b$. In the IR spectrum of [Cu(HAPO)Cl]($H_2O$), CS bands at the same position suggest that they do not participate in coordination and the disappearance of the band at 3363 $cm^{-1}$ due to the (C–OH) mode, in addition to a new band at 533 $cm^{-1}$ due to $\nu$(Cu–O), reveals this mode of coordination.

In all the complexes, a band at 480–424 $cm^{-1}$ assigned to $\nu$(Cu–N) supports the proposed mode of coordination. IR spectra of all complexes exhibit $\nu_{asym}$ and $\nu_{sym}$(OH) and $\Delta(H_2O)$ vibrations at ≈3399–3450 $cm^{-1}$ and a weak shoulder at 1625 $cm^{-1}$, respectively, suggesting water [36]. Broad bands at 875–850 $cm^{-1}$ and ≈540–550 refer to $P_r(H_2O)$ and $P_w(H_2O)$ vibrations and support that water is coordinated, confirmed by TGA studies.

### 3.3. *$^1$H NMR spectra*

$^1$H NMR spectra of $H_2PPS$, $H_2PBO$, $H_2APO$, and $H_2PPY$ in DMSO-$d_6$ show signals at $\delta$ = (10.30–10.90), (11.09–11.90), (8.09–8.25), (8.27–9.54), and (15.40, 15.80) ppm assignable to $(NH)_{a,,a'}$, $(NH)_{b,c}$, and SH protons, respectively. The peak of $(NH)_{a,,a'}$, disappears and the intensity of the $(NH)_{b,c}$ peak decreases on addition of $D_2O$, which suggests that they are easily exchangeable. These protons shift downfield because they hydrogen bond with N of pyridine and S of CS. The protons of $(NH)_a$ and $(NH)_{a'}$ appear as singlets as expected since the NH protons are decoupled from nitrogen and protons from adjacent atoms. $(NH)_b$ and $(NH)_c$ show coupling with the adjacent hydrogen as doublets. This coupling can be attributed to the low NH exchange rate. Signals attributed to pyridyl appear at $\delta$ = 8.26 (d, $J$ = 5.40 Hz, 1H, pyridine H6), 7.85 (dd, $J$ = 6.9, 5.4 Hz, 1H, pyridine H4), 7.65 (dd, $J$ = 6.9, 4.8 Hz, 1H, pyridine H5), and 7.35–7.50 (d, $J$ = 5.4 Hz, 1H, pyridine H3) for $H_2PPS$, 8.23 (dd, $J$ = 8.7 Hz, 1H, pyridine H5), 8.01 (d, $J$ = 5.3 Hz, 1H, pyridine H6), 7.9 (d, $J$ = 6.4 Hz, 1H, pyridine H3), 7.66 (dd, $J$ = 6.1 Hz, 1H, pyridine H4) for $H_2PBO$, 8.23 (dd, $J$ = 8.7 Hz, 1H, pyridine H5), 8.01 (d, $J$ = 5.3 Hz, 1H, pyridine H6), 7.9 (d, $J$ = 6.4 Hz, 1H, pyridine H3), 7.66 (dd, $J$ = 6.1 Hz, 1H, pyridine H4) for $H_2APO$, and 8.21 (d, $J$ = 6.2 Hz, 1H, pyridine H6), 8.17 (d, $J$ = 7.4 Hz, 1H, pyridine H3), 7.88 (dd, $J$ = 5.5 Hz, 1H, pyridine H5), 7.85 (dd, $J$ = 7.3 Hz, 1H, pyridine H4) for $H_2PPY$ [37]. The signal at $\delta$ (8.01–8.22) ppm for pyridine H6 in all thiosemicarbazides is superimposed with that of some NH $(NH)_{b,c}$ protons. Also, spectra of $H_2PPS$, $H_2PBO$, and $H_2APO$ at 7.00–7.64 ppm due to phenyl protons appear as complicated multiplets. A signal at $\delta$ 15.4 ppm in the spectrum of

Table 1. Magnetic moment and electronic spectra of the Cu(II) complexes of $H_2$PPS, $H_2$PBO, $H_2$APO, and $H_2$PPY.

| Compound | Solvent | Band position ($cm^{-1}$) | $\mu_{eff}$ (B.M.) |
|---|---|---|---|
| $H_2$PPS | DMF | 35,211; 31,847; 29,069 | – |
| | Nujol | – | |
| [Cu(HPPS)Cl($H_2O$)$_2$] | DMF | 35,211; 28,089; 26,178 18,587; 16,077 | 1.78 |
| | Nujol | 23,364; 20,408; 17,301 | |
| $H_2$PBO | DMF | 35,461; 32,680; 29,070 | – |
| | Nujol | – | |
| [Cu(HPBO)Cl($H_2O$)$_2$] | DMF | 32,258; 28,409; 18,050 | 2.03 |
| | Nujol | 25,000; 30,675; 17,606 | |
| $H_2$APO | DMF | 35,211; 32,051 | – |
| | Nujol | – | |
| [Cu(HAPO)Cl]($H_2O$) | DMF | 35,211; 32,467; 27,624 | 1.54 |
| | Nujol | 23,585; 19,685; 15,291 | |
| $H_2$PPY | DMF | 35,971; 28,409; 22,321 | |
| | Nujol | 35,211; 30,120; 18,050 | – |
| [Cu(HPPY)Cl($H_2O$)$_2$] | Nujol | 35,211; 31,847; 29,585 | |
| | DMF | 25,126; 19,157 | 1.83 |

$H_2$PPY due to SH and a signal at $\delta$ 12.80 ppm due to OH in $H_2$APO confirm the thiol–enol tautomerism in solution.

### 3.4. *Electronic spectra and magnetic moments*

The absorption bands and the magnetic moments of the thiosemicarbazides and their Cu(II) complexes in DMF and Nujol mull are recorded in table 1. The spectra exhibit bands at 35,111–35,971 $cm^{-1}$ and 30,120–32,680 $cm^{-1}$ assignable to $\pi \rightarrow \pi^*$ and $n \rightarrow \pi^*$ transitions, respectively [38]. Charge transfer is observed in spectra of complexes with a new $n \rightarrow \pi^*$ band at 28,089–29,585 $cm^{-1}$. The charge transfer band assigned to ($S \rightarrow Cu$) [38, 39] in [Cu(HPPS)Cl($H_2O$)$_2$], [Cu(HPBO)Cl($H_2O$)$_2$], and [Cu(HPPY)Cl($H_2O$)$_2$] appeared at higher energies (22,320–25,000 $cm^{-1}$) in Nujol possibly due to coordination *via* sulfur. The d–d transition bands for [Cu(HPPS)Cl($H_2O$)$_2$], [Cu(HPBO)Cl($H_2O$)$_2$], and [Cu(HPPY)Cl($H_2O$)$_2$] at 18,050–19,685 $cm^{-1}$ in DMF and at 17,301–18,116 $cm^{-1}$ in Nujol are consistent with octahedral complexes. For [Cu(HAPO)Cl]($H_2O$), the band due to d–d transition appeared at 15291 $cm^{-1}$ in DMF confirming a square-planar environment. These geometries will be further confirmed by ESR spectra. Magnetic moment values fall in the range reported for $d^9$ Cu(II) complexes.

### 3.5. *ESR spectra*

ESR spectra of Cu(II) complexes provide information about hyperfine and super-hyperfine structures which are important in studying the metal ion environment in

Table 2. ESR data of some Cu(II) complexes at room temperature.

| Complex | $g_{\parallel}$ | $g_{\perp}$ | $A_{\parallel} \times 10^{-4}$ ($cm^{-1}$) | $G$ | $g_{\parallel}/A_{\parallel}$ | $\alpha^2$ | $\beta^2$ |
|---|---|---|---|---|---|---|---|
| [Cu(HPPS)Cl($H_2O$)] | 2.28 | 2.06 | 165 | 4.60 | 138 | 0.80 | 0.90 |
| [Cu(HPBO)Cl($H_2O$)]($H_2O$) | 2.29 | 2.06 | 168 | 3.30 | 136 | 0.73 | 0.74 |
| [Cu(HAPO)Cl]($H_2O$)$_3$ | 2.25 | 2.08 | – | 3.12 | – | – | – |
| [Cu(HPPY)Cl($H_2O$)]($H_2O$) | 2.23 | 2.07 | 150 | 3.20 | 148 | 0.71 | 0.87 |



complexes, i.e., the geometry, nature of the ligation sites and degree of covalency of the metal ligand bonds (Supplementary material). The spin Hamiltonian parameters of the complexes with Cu(II), $S = 1/2$, $I = 3/2$, were calculated and are summarized in table 2.

Room temperature solid state ESR spectra of these complexes are similar and exhibit axially symmetric $g$-tensor parameters with $g_{\parallel} > g_{\perp} > 2.0023$ revealing an appreciable covalency with $d_{(x2-y2)}$ as the ground-state [40], characteristic of square-planar, square-pyramidal or octahedral stereochemistry [41].

In axial symmetry the $g$-values are related by the expression $G = (g_{\parallel} - 2)/(g_{\perp} - 2) = 4$, where $G$ is the exchange interaction parameter. According to Hathaway and Billing [42], if $G$ is greater than 4, the exchange interaction between copper(II) centers in the solid state is negligible, whereas when it is less than 4, considerable exchange interaction is indicated. The calculated $G$ values (Supplementary material) show $G > 4$ for [Cu(HPPS)Cl($H_2O$)$_2$] and less than 4 for [Cu(HPBO)Cl($H_2O$)$_2$], [Cu(HAPO)Cl]($H_2O$), and [Cu(HPPY)Cl($H_2O$)$_2$] [43].

A band corresponding to forbidden magnetic dipolar transition for [Cu(HPBO)Cl($H_2O$)$_2$], [Cu(HPPS)Cl($H_2O$)$_2$], and [Cu(HPPY)Cl($H_2O$)$_2$] is not observed at half-field (*ca* 1600 $G$, $g = 4.0$), revealing mononuclear Cu(II) complexes [44]. Superhyperfine structures for these complexes are not seen at higher fields excluding any interaction of the nuclear spins of nitrogen ($I = 1$) with the unpaired electron density on Cu(II).

The absorption for [Cu(HAPO)Cl]($H_2O$) consists of a broad band centered at $g = 2$, attributable to dipolar broadening and enhanced spin lattice relaxation [45]. This line broadening is probably due to insufficient spin exchange narrowing toward the coalescence of four copper hyperfine lines to a single line; similar powder ESR line shapes have been observed for many square-planar or distorted octahedral dimeric Cu(II) complexes with strong intra-dimer spin-exchange interaction [46]. Hyperfine splitting due to the spin of copper was not detected because of the broadness. These observations confirm occurrence of super exchange coupling between Cu(II) ions in the dimeric complexes, consistent with the subnormal effective magnetic moment values which may refer to sulfur coordination [47].

The tendency of $A_{\parallel}$ to decrease with concomitant increase of $g_{\parallel}$ is an index of tetrahedral distortion in the coordination sphere of copper. To quantify the degree of distortion of the Cu(II) complexes, we selected $f(\alpha) = g_{\parallel}/A_{\parallel}$ obtained from the ESR spectra. Values of 110–120 are typical for planar complexes, while the range 130–150 is characteristic of slight to moderate distortion and 180–250 $cm^{-1}$ indicate considerable distortion [48, 49]. The ratio $g_{\parallel}/A_{\parallel}$ for [Cu(HPBO)Cl($H_2O$)$_2$], [Cu(HPPS)Cl($H_2O$)$_2$], and [Cu(HPPY)Cl($H_2O$)$_2$] are 136, 138, and 148, respectively, demonstrating significant dihedral angle distortion in the $xy$-plane, consistent with distorted octahedral geometry around the copper site.

Molecular orbital coefficients, $\alpha^2$ (a measure of the covalency of the in-plane $\sigma$-bonding between a copper 3d orbital and the ligand orbitals) and $\beta^2$ (covalent in-plane $\pi$-bonding), were calculated by using the following equations [50–53]:

$$\alpha^2 = \left(A_{\parallel}/0.036\right) + \left(g_{\parallel} - 2.0023\right) + 3/7(g_{\perp} - 2.0023) + 0.04,$$
$$\beta^2 = \left(g_{\parallel} - 2.0023\right)E/ - 8\lambda\alpha^2,$$

where $\lambda = -828\,\mathrm{cm}^{-1}$ for free copper ion and $E$ is the electronic transition energy.

As a measure of the covalency of the in-plane $\sigma$-bonding, $\alpha^2 = 1$ indicates complete ionic character, whereas $\alpha^2 = 0.5$ denotes 100% covalent bonding with the assumption of negligibly small values of overlap integral. $\beta^2$ gives an indication of the covalency of the in-plane $\pi$-bonding. The smaller $\beta^2$, the larger is the covalency of the bonding.

Values of $\alpha^2$ and $\beta^2$ for [Cu(HPBO)Cl($H_2O$)$_2$], [Cu(HPPS)Cl($H_2O$)$_2$], and [Cu(HPPY)Cl($H_2O$)$_2$] indicate that the in-plane $\sigma$-bonding and in-plane $\pi$-bonding are covalent, which originates from thiolato sulfur binding incorporating greater covalency in the metal–ligand bonding through delocalized $d_\pi$–$p_\pi$ in-plane $\pi$-bonding as evidenced from higher $\beta^2$ values [54]. Data for [Cu(HAPO)Cl]($H_2O$) show that in-plane $\sigma$-bonding and in-plane $\pi$-bonding are ionic. For square-planar geometry, the lower values of $\beta_2$ compared to $\alpha_2$ indicate that in-plane $\pi$-bonding is more covalent than the in-plane $\sigma$-bonding, consistent with other reported values [55–58].

### 3.6. *Molecular modeling*

The molecular structure and atom-numbering of ligands and its Cu(II) complex are shown in schemes 1–8.

From data recorded in Supplementary tables (S1–S9) for bond lengths and angles, one can conclude the following: (1) bond angles of the thiosemicarbazide are altered upon coordination with largest effects on S(9)–C(8)–N(10), C(8)–N(10)–N(11), N(10)–N(11)–C(12), and C(4)–N(7)–C(8) angles which are reduced from 123.3°, 116.8°, 123.3°, and 127.6° in $H_2$PPS to 97.6°, 127.5°, 107.5°, and 106° for [Cu(HPPS)Cl($H_2O$)$_2$]; N(10)–N(11)–C(12) and N(11)–C(12)–S(13) from 124° and 126.1° in $H_2$PBO to 115° and 119.6° for [Cu(HPBO)Cl($H_2O$)$_2$]; C(5)–C(4)–N(7) and N(10)–N(11)–C(12) from 126.6° and 122.5° in $H_2$APO to 121.6° and 114.3° for [Cu(HAPO)Cl]($H_2O$), and N(11)–C(12)–S(13) and N(11)–C(12)–N(14) from 123.6° and 115.6° in $H_2$PPY to 118.4° and 122.5° for [Cu(HPPY)Cl($H_2O$)$_2$] [59]. (2) All bond angles in the complexes are close to octahedral geometry except for [Cu(HAPO)Cl]($H_2O$), which has a square-planar geometry. (3) All groups taking part in coordination, C=S, N–H, $(C{=}N)_{py}$, and (C=O), have bonds longer than in the ligand. (4) The presence of two water molecules in *trans* position for [Cu(HPPY)Cl($H_2O$)$_2$]. (5) Lower highest occupied molecular orbital (HOMO) energy values show weaker electron donation while higher HOMO energy implies a good electron donor. Lowest unoccupied molecular orbital energy represents the ability of a molecule receiving electron [60].

### 3.7. *Thermogravimetric studies*

The stages of decomposition, temperature range, decomposition product, and weight loss percentages of complexes are given in table 3. A glance at the table indicates that

Table 3. Decomposition steps with temperature range and weight loss for ligands and their copper complexes.

| Compound | Temperature range (°C) | Removed species | Weight loss | |
|---|---|---|---|---|
| | | | Found (%) | Calcd (%) |
| $H_2PPS$ | 141–228 | $-Py + NH$ | 30.84 | 30.68 |
| | 229–371 | $-Py + NH + CS$ | 45.76 | 45.18 |
| | 513–691 | $-N_2H_2$ | 9.58 | 9.8 |
| | 691–800 | CS (residue) | 13.8 | 14.5 |
| $[Cu(HPPS)Cl(H_2O)_2]$ | 190–279 | $-2H_2O + HCl$ | 16.78 | 16.57 |
| | 280–390 | $-Py$ | 17.65 | 17.85 |
| | 391–527 | $-CN$ | 5.85 | 5.95 |
| | 528–754 | $-CN_2H + NH + Ph$ | 30.17 | 30.44 |
| | 754–800 | $CuS + S$ (residue) | 29.55 | 29.19 |
| $H_2PBO$ | 0–210 | $-Py + NH$ | 28.58 | 28.09 |
| | 210–370 | $-C_3H_3S_2O$ | 48.16 | 48.64 |
| | 370–700 | $C_6H_5$ | 23.28 | 23.27 |
| $[Cu(HPBO)Cl(H_2O)_2]$ | 188–292 | $-2H_2O$ | 7.87 | 7.94 |
| | 292–441 | $-Cl + Py + N_2H_2 + 2C$ | 35.65 | 35.85 |
| | 441–695 | $-C_6H_5 + NH + N + C$ | 25.69 | 25.37 |
| | 695–800 | $CuO + 2S$ (residue) | 30.79 | 30.84 |
| $H_2APO$ | 126–217 | $-C_5H_5N_2 + N_2H_2$ | 42.15 | 42.85 |
| | 217–344 | $-C_6H_5 + CO + NH$ | 41.11 | 41.82 |
| | 344–700 | CS (residue) | 16.74 | 15.34 |
| $[Cu(HAPO)Cl](H_2O)$ | 21–137 | $-H_2O$ | 4.03 | 4.47 |
| | 137–258 | $-Py + Cl + NH$ | 31.77 | 31.88 |
| | 258–397 | $-C_6H_5$ | 19.63 | 19.12 |
| | 397–570 | $-NH + C$ | 6.51 | 6.69 |
| | 570–776 | $-N_2H + C$ | 10.93 | 10.17 |
| | 776–800 | $CuO + S$ (residue) | 27.13 | 27.8 |
| $H_2PPY$ | 188–246 | $-N_2H_2$ | 10.57 | 9.86 |
| | 246–400 | $-2Py + N_2H_2$ | 60.96 | 61.18 |
| | 400–700 | 2CS (residue) | 28.78 | 28.96 |
| $[Cu(HPPY)Cl(H_2O)_2]$ | 290–467 | $-2H_2O + Cl$ | 16.71 | 16.30 |
| | 467–660 | $-2Py + N_4H_3 + 2C$ | 54.16 | 54.56 |
| | 660–800 | $Cu + 2S$ (residue) | 29.13 | 29.12 |



thermal stabilities of ligands increase on complex formation. TGA curves of $[Cu(HPPS)Cl(H_2O)_2]$ as a representative example (Supplementary material) display five degradation steps. The first at 190–279°C with weight loss of 16.78 (Calcd 16.57%) is attributed to loss of the two lattice water molecules and Cl. The second step with weight loss of 17.65 (Calcd 17.85%) at 280–390°C corresponds to removal of pyridine. The third step at 391–557°C with weight loss of 5.85 (Calcd 5.95%) is for removal of CN. The fourth step (558–754°C) can be ascribed to elimination of $CN_4H$ fragment with weight loss of 30.17 (Calcd 30.44%). The residual is $CuS + S$ (found 29.55, Calcd 29.19%).

### 3.8. *pH metric studies*

The average number of protons associated with ligand $\bar{n}_a$ was calculated at different pH-values using the Irving–Rossotti equation [61] and used to draw proton-ligand

formation curves, which indicated that the maximum $n_a$ is ~2 revealing that the investigated ligands have two dissociable protons of $NH^b$ and $NH^c$, respectively. An inspection of the results in table 4 reveals the following:

(1) **Effect of substituent:** p$K_1$ values of the ligands are influenced by the inductive effect of the substituent. The p$K$ values under the same conditions of temperature and ionic strength can be arranged as $H_2$APO > $H_2$PPS > $H_2$PPY > $H_2$PBO, attributed to hydrogen-bond formation. The first three compounds form two hydrogen bonds and the last one forms three hydrogen bonds, and as a result it is difficult to lose $H^+$, so the p$K$ is high. On substituting carbonyl by thione, the p$K$ value decreases as oxygen is more electronegative than sulfur. The presence of pyridyl in $H_2$PPY (i.e., electron withdrawing) decreases the electron density more effectively than phenyl, giving a stronger hydrogen bond and, consequently, smaller p$K$.
(2) **Effect of ionic strength:** There is an increase in p$K$ with increasing ionic strength of the medium, consistent with that reported [62].
(3) **Effect of temperature:** p$K_a$ values decrease with increasing temperature, i.e., the acidity of ligands increase with increasing temperature.
(4) **The stepwise stability constants of complexes:** The values (table 5) decrease with increasing temperature, indicating that complexation is unfavorable with increasing temperature.
(5) **Thermodynamic parameters:** $\Delta G^\circ$ values are positive, indicating non-spontaneous character of the dissociation processes. $\Delta S^\circ$ values were negative, indicating that dissociation is entropically unfavorable due to disorder of the solvent around the ligand [63]. Positive values of $\Delta H^\circ$ indicate that dissociation of ligands is endothermic.

"Supplementary material" shows that $\Delta G^\circ$ values are negative, indicating spontaneous chelation. Negative values of $\Delta S^\circ$ indicate that complexation is entropically unfavorable while negative values of $\Delta H^\circ$ suggest that chelation is accompanied by generation of heat, indicating that the processes are exothermic, i.e., complexation is favorable at lower temperature.

### 3.9. *DNA degradation studies*

DNA cleavage reactions generally occur through three pathways, namely oxidative strand cleavage by abstraction of a sugar hydrogen (s), hydrolytic cleavage involving the phosphate, and by base oxidations primarily directed at guanine. Irradiation is one methodology for inducing DNA cleavage [64]. For the sulfur containing thiosemicarbazides thio or thione moieties exhibit efficient intersystem crossing to the triplet state $^3(n$–$\pi^*)$ and/or $^3(\pi$–$\pi^*)$. Such state with a longer lifetime can either cause damage to DNA directly or can activate oxygen from its triplet state ($^3O_2$) to the cytotoxic singlet state ($^1O_2$) [65, 66]. Examining DNA degradation assay for $H_2$PPS, $H_2$PBO, $H_2$APO, and $H_2$PPY, and their corresponding Cu(II) complexes revealed variability on their immediate damage on the ct-DNA (figure 1). The results show that either DNA in DMF (+ve control) or DNA treated with **2**, **3**, **4**, and **5** showed no effect through the incubation period, whereas **6** exhibited partial degradation, judged by the rate of DNA migration in the gel. DNA disappeared completely after treatment with **7**, **8**, and **9** due to direct contact of these complexes with DNA, which is necessary to degrade it. The

Table 4. The dissociation constants of $H_2PPS$ in 50% (v/v) dioxane-water and KCl at different temperatures and their thermodynamic parameters.

| | | Dissociation constant | | | | | | Free energy change ($\Delta G$) (kJ mol$^{-1}$) | | | | | | | | | |
|---|---|---|---|---|---|---|---|---|---|---|---|---|---|---|---|---|---|
| | | 298 K | | 303 K | | 308 K | | | | | | | | | | | |
| Compound | $\mu$ (mol L$^{-1}$) | p$K$1 | p$K$2 | p$K$1 | p$K$2 | p$K$1 | p$K$2 | 298 K | | 303 K | | 308 K | | Enthalpy change ($\Delta H$) (kJ mol$^{-1}$) | | Entropy change ($\Delta S$) (J mol$^{-1}$ K$^{-1}$) | |
| $H_2PPS$ | 0.1 | 13.45 | 8.25 | 12.89 | 8.15 | 8.72 | 6.76 | 82.7 | 24.8 | 83.3 | 25.0 | 83.9 | 25.2 | 43.37 | 13.66 | −131.9 | −37.55 |
| | 0.15 | 13.44 | 10.2 | 11.98 | 8.56 | 11.8 | 7.88 | 26.1 | 21.7 | 26.3 | 39.9 | 27.5 | 40.2 | 15.06 | 21.29 | −37.12 | −61.28 |
| | 0.2 | 12.90 | 7.80 | 10.88 | 7.26 | 9.25 | 4.35 | 63.2 | 60.9 | 63.7 | 61.4 | 64.2 | 61.9 | 33.50 | 31.63 | −99.57 | −98.30 |
| $H_2PBO$ | 0.1 | 12.89 | 8.99 | 10.51 | 8.15 | 10.02 | 7.60 | 48.9 | 22.8 | 49.3 | 23.0 | 51.9 | 23.2 | 26.35 | 12.77 | −75.58 | −33.89 |
| | 0.15 | 12.98 | 9.02 | 11.6 | 8.55 | 11.57 | 7.36 | 22.0 | 27.7 | 22.2 | 27.9 | 22.3 | 28.2 | 12.94 | 15.22 | −30.46 | −42.00 |
| | 0.2 | 12.49 | 7.52 | 10.46 | 7.41 | 9.80 | 6.48 | 45.7 | 16.8 | 46.0 | 16.9 | 46.4 | 17.1 | 24.69 | 9.53 | −70.41 | −24.44 |
| $H_2ABO$ | 0.1 | 14.00 | 8.48 | 13.54 | 8.04 | 10.98 | 6.03 | 51.2 | 42.4 | 27.7 | 42.7 | 51.9 | 43.0 | 27.67 | 22.46 | −78.75 | −66.85 |
| | 0.15 | 13.65 | 9.05 | 10.81 | 8.33 | 9.93 | 5.30 | 64.2 | 66.4 | 64.7 | 66.9 | 65.2 | 67.4 | 34.14 | 34.73 | −100.9 | −106.2 |
| | 0.2 | 13.36 | 8.64 | 9.60 | 7.41 | 9.41 | 6.64 | 68.5 | 34.2 | 69.1 | 34.4 | 69.6 | 34.7 | 36.25 | 18.36 | −108.3 | −53.04 |
| $H_2PPY$ | 0.1 | 13.04 | 9.00 | 12.33 | 8.47 | 9.93 | 6.65 | 53.1 | 40.4 | 53.5 | 40.7 | 53.9 | 41.0 | 28.51 | 21.54 | −82.54 | −63.23 |
| | 0.15 | 14.25 | 8.65 | 11.47 | 7.77 | 8.85 | 4.22 | 94.8 | 78.6 | 95.6 | 79.3 | 96.3 | 79.9 | 49.54 | 40.62 | −152.0 | −127.6 |
| | 0.2 | 11.85 | 8.75 | 9.92 | 7.55 | 8.84 | 6.19 | 51.8 | 44.3 | 52.2 | 44.7 | 52.6 | 45.0 | 27.63 | 23.48 | −80.94 | −69.99 |

Table 5. The stability constants of Cu(II) complexes in 50% (v/v) dioxane-water and KCl at different temperatures.

| | | Dissociation constant | | | | | |
|---|---|---|---|---|---|---|---|
| | | 298 K | | 303 K | | 308 K | |
| Compound | $\mu$ (mol $L^{-1}$) | log *K*1 | log *K*2 | log *K*1 | log *K*2 | log *K*1 | log *K*2 |
| Cu(II) + $H_2$PPS | 0.1 | 18.58 | 11.30 | 16.83 | 9.77 | 11.36 | 3.32 |
| | 0.15 | – | 7.36 | – | 14.16 | – | 9.93 |
| | 0.2 | 16.20 | 10.98 | 14.87 | 8.59 | – | 6.57 |
| Cu(II) + $H_2$PBO | 0.1 | 17.71 | 6.91 | 15.42 | 6.38 | 14.01 | 3.96 |
| | 0.15 | 18.72 | 9.85 | – | 12.43 | – | 13.21 |
| | 0.2 | – | 13.31 | – | 12.07 | – | 13.80 |
| Cu(II) + $H_2$APO | 0.1 | 18.42 | 9.75 | 16.06 | 8.92 | 14.91 | 6.43 |
| | 0.15 | 12.52 | 7.65 | – | 12.29 | 9.16 | 6.96 |
| | 0.2 | 15.93 | 10.31 | – | 11.16 | – | 10.74 |
| Cu(II) + $H_2$PPY | 0.1 | 19.70 | 11.20 | 16.29 | 8.34 | 15.43 | 8.23 |
| | 0.15 | 14.68 | – | 13.37 | – | – | 7.47 |
| | 0.2 | 14.45 | 10.64 | 13.98 | 11.38 | – | 6.49 |

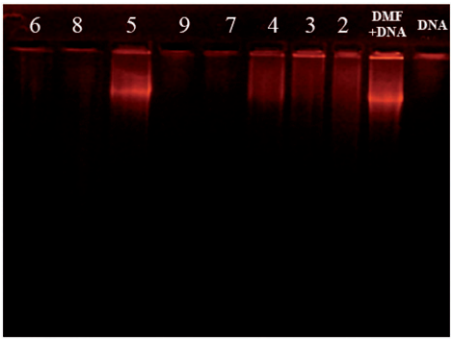


Figure 1. Effect of free ligands and their Cu(II) complexes on the DNA *in vitro*.

data suggest that conjugation between the thio and imine make them inefficient, possibly by reducing the triplet state ($n$–$\pi^*$) and/or the $^3(\pi$–$\pi^*)$ lifetime of the sulfur ligand in an enolic form. The absence of such conjugation in **6**, **7**, **8**, and **9** in addition to the near planarity of the chelate ring enhances the photosensitization and consequently can either cause damage of DNA directly or activate oxygen. Therefore, **7** and **8** can be used as a promising anti-tumor agent *in vivo* to inhibit the DNA replication in the cancer cells and not allow the tumor to further grow [67].

## 4. Conclusion

Based on the elemental analysis and spectral data for Cu(II) complexes of $H_2$PPS, $H_2$PBO, $H_2$APO, and $H_2$PPY, the substituents modify the coordination. The ligands

coordinate to copper as SN bidentate, NON tridentate, or NSNS tetradendate, forming structures in which each copper is square-planar or octahedral. ESR spectra of these complexes are quite similar, exhibiting axially symmetric $g$-tensor parameters with $g_{\parallel} > g_{\perp} > 2.0023$ revealing $d_{(x^2-y^2)}$ as ground-state. Thermal degradation indicated high stability of the formed chelates. Also, pH-metric studies were carried out at different temperatures and ionic strengths, and revealed the effect of the substituent on the dissociation constants of the thiosemicarbazides. At a given temperature, p$K$ values are in the order $H_2APO > H_2PPS > H_2PPY > H_2PBO$. DNA degradation assay for $H_2PPS$, $H_2PBO$, $H_2APO$, and $H_2PPY$ and their corresponding Cu(II) complexes showed that the existence of conjugation in the thiosemicarbazides reduced the triplet state lifetime of the sulfur ligand in the thiol form, so they were unable to cause damage on DNA. Absence of such conjugation in the Cu(II) complexes enhanced their ability to cause DNA cleavage. $[Cu(HPBO)Cl(H_2O)](H_2O)$ and $[Cu(HAPO)Cl](H_2O)_3$ have the highest degradation ability.



## References


[1] D.X. West, S.B. Padhyé, P.B. Sonawane. *Struct. Bond.*, **76**, 1 (1991).
[2] D.X. West, A.E. Liberta, S.B. Padhyé, R.C. Chikate, P.B. Sonawane, A.S. Kumbhar, R.G. Yerande. *Coord. Chem. Rev.*, **123**, 49 (1993).
[3] M.B. Ferrari, G.G. Fava, E. Lepoati, G. Pelosi, R. Rossi, P. Tarasconi, R. Albertini, A. Boati, P. Lunghi, S. Pinelli. *J. Inorg. Biochem.*, **70**, 145 (1998).
[4] P.B. Sonawane, R.C. Chikate, A.S. Kumbhar, S.B. Padhyé, R.J. Doedens. *Polyhedron*, **13**, 195 (1994).
[5] A.M. Thomas, A.D. Naik, M. Nethaji, A.R. Chakravarty. *Inorg. Chim. Acta*, **357**, 2315 (2004).
[6] M. Belicchi-Ferrari, F. Bisceglie, G. Pelosi, P. Tarasconi. *Polyhedron*, **27**, 1361 (2008).
[7] P.E. Rapheal, E. Manoj, M.R. Prathapachandra Kurup. *Polyhedron*, **26**, 818 (2007).
[8] H. Beraldo, D. Gambino. *Min. Rev. Med. Chem.*, **4**, 31 (2004).
[9] M.B. Ferrari, F. Bisceglie, G.G. Fava, G. Pelosi, P. Tarasconi, R. Albertini, S. Pinelli. *J. Inorg. Biochem.*, **89**, 36 (2002).
[10] H.S. Seleem, B.A. El-Shetary, S.M.E. Khalil, M. Mostafa, M. Shebl. *J. Coord. Chem.*, **58**, 479 (2005).
[11] J.R.J. Sorenson. *Prog. Med. Chem.*, **26**, 437 (1989).
[12] M. Kato, Y. Muto. *Coord. Chem. Rev.*, **92**, 45 (1988).
[13] J.E. Weder, C.T. Dillon, T.W. Hambley, B.J. Kennedy, P.A. Lay, J.R. Biffin, H.L. Regtop, N.M. Davies. *Coord. Chem. Rev.*, **232**, 95 (2002).
[14] G. Psomas, A. Tarushi, E.K. Efthimiadou, Y. Aanakis, C.P. Raptopoulou, N. Katsaros. *J. Inorg. Biochem.*, **100**, 1764 (2006).
[15] D.S. Sigman, D.R. Graham, V.D. Aurora, A.M. Stern. *J. Biol. Chem.*, **254**, 12269 (1979).
[16] F.Q. Liu, Q. Wang, K. Jiao, F. Jian, G. Liu, R. Li. *Inorg. Chim. Acta*, **359**, 1524 (2006).
[17] M.M. Meijler, O. Zelenko, D.S. Sigman. *J. Am. Chem. Soc.*, **119**, 1135 (1997).
[18] S.A. Ross, M. Pitié, B. Meunier. *Eur. J. Inorg. Chem.*, **1999**, 557 (1999).
[19] G. Psomas, C.P. Raptopoulou, L. Iordanidis, C. Dendrinou-Samara, V. Tangoulis, D.P. Kessissoglou. *Inorg. Chem.*, **39**, 3042 (2000).
[20] C. Dendrinou-Samara, G. Psomas, C.P. Raptopoulou, D.P. Kessissoglou. *J. Inorg. Biochem.*, **83**, 7 (2001).
[21] B.K. Santra, P.A.N. Reddy, G. Neelakanta, S. Mahadevan, M. Nethaji, A.R. Chakravartym. *J. Inorg. Biochem.*, **89**, 91 (2002).
[22] L.Z. Li, C. Zhao, T. Xu, H. Ji, Y. Yu, G. Guo, H. Chao. *J. Inorg. Biochem.*, **99**, 1076 (2005).
[23] K.K. Du, S.X. Liu. *J. Mol. Struct.*, **874**, 138 (2008).
[24] L.G. Van Uitert, C. Hass. *J. Am. Chem. Soc.*, **75**, 365 (1953).
[25] J. Sambrook, E.F. Fritsh, T. Maniatis. *Molecular Cloning: A Laboratory Manual*, Cold Spring Harbor Laboratory Press, Cold Spring Harbor, NY (1989).
[26] N.L. Allinger. *J. Am. Chem. Soc.*, **99**, 8127 (1977).
[27] *HyperChem (Version 8.0.3)*. Available online at: www.hyper.com (2007).
[28] T.A. Yousef, F.A. Badria, S.E. Ghazy, O.A. El-Gammal, G.M. Abu El-Reash. *Inter. J. Med. Medical Sci.*, **3**, 37 (2001).

[29] D.X. West, G. Ertem, M. Patricia, J.P. Scovill, D.L. Klayman, L. Judith, F. Anderson, R. Gillardi, C. George, L.K. Pannel. *Trans. Met. Chem.*, **10**, 264 (1985).
[30] Z. Li, Y. Zhang, Y. Wang. *Phosphorous, Sulphur, Silicon Relat. Elem.*, **178**, 293 (2003).
[31] A. Braibanti, F. Delavalla, M.E. Pellinghelli, E. Laporti. *Inorg. Chem.*, **7**, 430 (1968).
[32] I.M. Bazova, R.G. Dubenkon, P.S. Pel'kis. *J. Organ. Khimii*, **14**, 195 (1976); *Chem. Abstr.*, **84**, 105468w (1976).
[33] D.K. Rastoh, K.C. Sharma. *J. Inorg. Nucl. Chem.*, **36**, 2219 (1974).
[34] M.J.M. Campbell. *Coord. Chem. Rev.*, **15**, 279 (1975).
[35] R. Mayer, M. Jansen (Eds). *Organosulfur Chemistry*, Interscience, New York (1967).
[36] M.S. Refat. *J. Mol. Struct.*, **842**, 24 (2007).
[37] R. Carpignano, P. Savarino, E. Barni, G. Viscardi. *J. Heterocyl. Chem.*, **21**, 561 (1984).
[38] F.A. El-Saied, A.A. El-Asmy, W. Kaminstry, D.X. West. *Trans. Met. Chem.*, **28**, 954 (2003).
[39] S. Delgado, M. Moran, U. Fernandez. *J. Coord. Chem.*, **12**, 105 (1982).
[40] D. Kivelson, R. Niemen. *J. Chem. Phys.*, **35**, 149 (1961).
[41] G. Speie, J. Csihony, A.M. Whalen, C.G. Pie-pont. *Inorg. Chem.*, **35**, 3519 (1996).
[42] B.J. Hathaway, D.E. Billing. *Coord. Chem. Rev.*, **5**, 143 (1970).
[43] J.L. Mesa, J.L. Pizarro, M.I. Arriortua. *Cryst. Res. Technol.*, **33**, 3 (1998).
[44] V.T. Kasumo. *Spectrochim. Acta, Part A*, **57**, 1649 (2001).
[45] (a) H. Yokoi, M. Chikira. *J. Am. Chem. Soc.*, **97**, 3975 (1975); (b) V.H. Growford, W.E. Hatfield. *Inorg. Chem.*, **16**, 1336 (1977).
[46] S. Pal. *Proc. Ind. Acad. Sci. (Chem. Sci.)*, **114**, 417 (2002).
[47] O. Khan, T. Mallah, J. Gouteron, S. Jeanin, Y.J. Eanin. *J. Chem. Soc., Dalton Trans.*, 1117 (1989).
[48] A.W. Addison. In *Spectroscopic and Redox Trends from Model Copper Complexes*, K.D. Karlin, J. Zubieta (Eds), p. 460, Adenine Press, New York (1983).
[49] V.V. Pavlischuk. *Theor. Exp. Chem.*, **31**, 1 (1995).
[50] R.K. Ray, G.R. Kauffman. *Inorg. Chim. Acta*, **173**, 207 (1990).
[51] K. Jayasubramanian, S.A. Samath, S. Thambidurai, R. Murugesan, S.K. Ramalingam. *Trans. Met. Chem.*, **20**, 76 (1995).
[52] V.S.X. Anthonisamy, R. Murugesan. *Chem. Phys. Lett.*, **287**, 353 (1998).
[53] V.S.X. Anthonisamy, R. Anantharam, R. Murugesan. *Spectrochim. Acta, Part A*, **55**, 135 (1999).
[54] R.C. Chikate, A.R. Belapure, S.B. Padhye, D.X. West. *Polyhedron*, **24**, 889 (2005).
[55] N. Raman, Y.P. Raja, A. Kulandaisamy. *Proc. Ind. Acad. Sci. (Chem. Sci.)*, **113**, 183 (2001).
[56] R.P. John. *Spectrochim. Acta, Part A*, **59**, 1349 (2003).
[57] G.A.A. Al-Hazmi, M.S. El-Shahawi, E.M. Gabr, A.A. El-Asmy. *J. Coord. Chem.*, **58**, 713 (2005).
[58] N.M. El-Metwally, E.M. Gabr, A.A. Abou-Hussen, A.A. El-Asmy. *Trans. Met. Chem.*, **31**, 71 (2006).
[59] O.A. El-Gammal. *Spectrochim. Acta, Part A*, **75**, 533 (2010).
[60] S. Sagdinc, B. Koksoy, F. Kandemirli, S.H. Bayari. *J. Mol Struct.*, **917**, 63 (2009).
[61] H.M. Irving, H.S. Rossotti. *J. Chem. Soc.*, 2904 (1954).
[62] M. Jelikic, D. Veselinovic, P. Djurdevic. *Talanta*, **59**, 655 (1992).
[63] M.G. Abd El-Wahed, S.M. Metwally, M.M. El-Gamel, S.M. Abd El-Haleem. *Bull. Kor. Chem. Soc.*, **22**, 663 (2001).
[64] A.M. Thomas, A.D. Naik, M. Nethaji, A.R. Chakravarty. *Inorg. Chim. Acta*, **357**, 2314 (2004).
[65] M. Baldini, M.B. Ferrari, F. Bisceglie, G. Pelosi, S. Pinelli, P. Tarasconi. *J. Inorg. Chem.*, **42**, 2049 (2003).
[66] Q. Xuhong, H. Tian-Bao, W. Dong-Zhi, Z. Dong-Hui, F. Mingcai, V. Wei. *J. Chem. Soc., Perkin Trans.*, **2**, 715 (2000).
[67] U. El-Ayaan, M.M. Youssef, S. Al-Shihry. *J. Mol. Struct.*, **936**, 213 (2009).